

Supporting Information

Label-Free Optical Detection of DNA Translocations Through Plasmonic Nanopores

Daniel V. Verschueren¹, Sergii Pud¹, Xin Shi^{1,2}, Lorenzo De Angelis³, L. Kuipers³, and Cees Dekker^{1,}*

¹Department of Bionanoscience, Kavli Institute of Nanoscience, Delft University of Technology, Van der Maasweg 9, 2629 HZ, Delft, The Netherlands

²Key Laboratory for Advanced Materials & School of Chemistry and Molecular Engineering, East China University of Science and Technology, Shanghai, 200237, P. R. China.

³Department of Quantum Nanoscience, Kavli Institute of Nanoscience, Delft University of Technology, Lorentzweg 1, 2628 CJ, Delft, The Netherlands

*E-mail: c.dekker@tudelft.nl

Table of Contents

- S1. Additional TEM images of inverted-bowtie plasmonic nanopores
- S2. Experimental and simulated spectrum of plasmonic nanopore
- S3. Simulation of idealized inverted-bowtie nanoantenna in transverse polarization
- S4. Experimental and simulated temperature increase in a plasmonic nanopore
- S5. Blockade current *versus* dwell time scatter plots
- S6. All-point histograms of optically detected events at different bias voltages
- S7. Simulation of the normalized electric field across the gold nanoantenna gap
- S8. Details on the determination of the relative simulated signal amplitude

S1. Additional TEM images of inverted-bowtie plasmonic nanopores

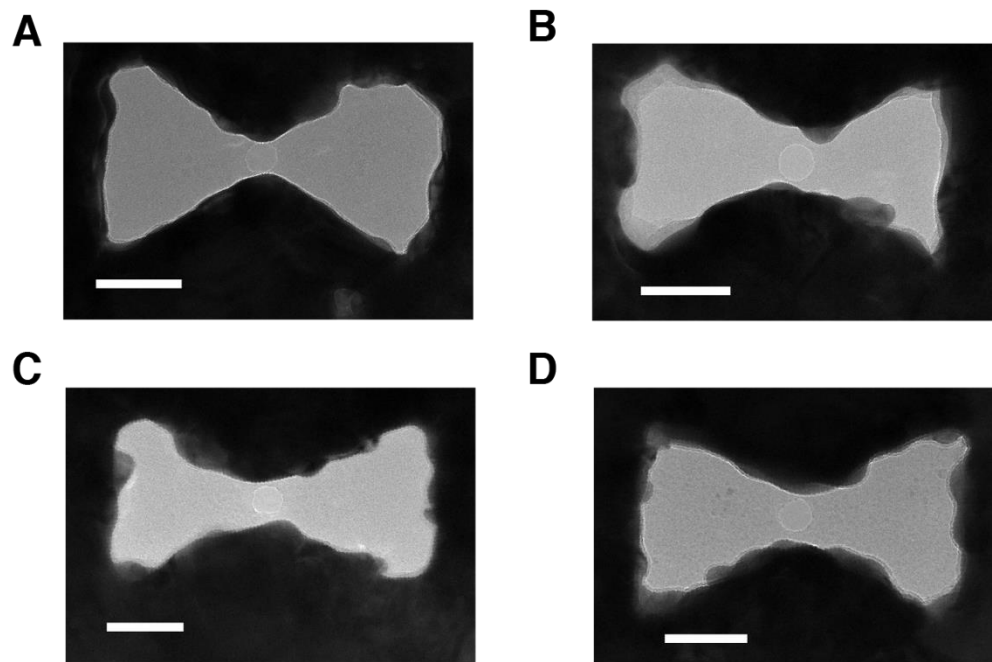


Figure S1. Additional TEM images of plasmonic nanopores. Scale bars are 50 nm.

S2. Experimental and simulated spectrum of plasmonic nanopore

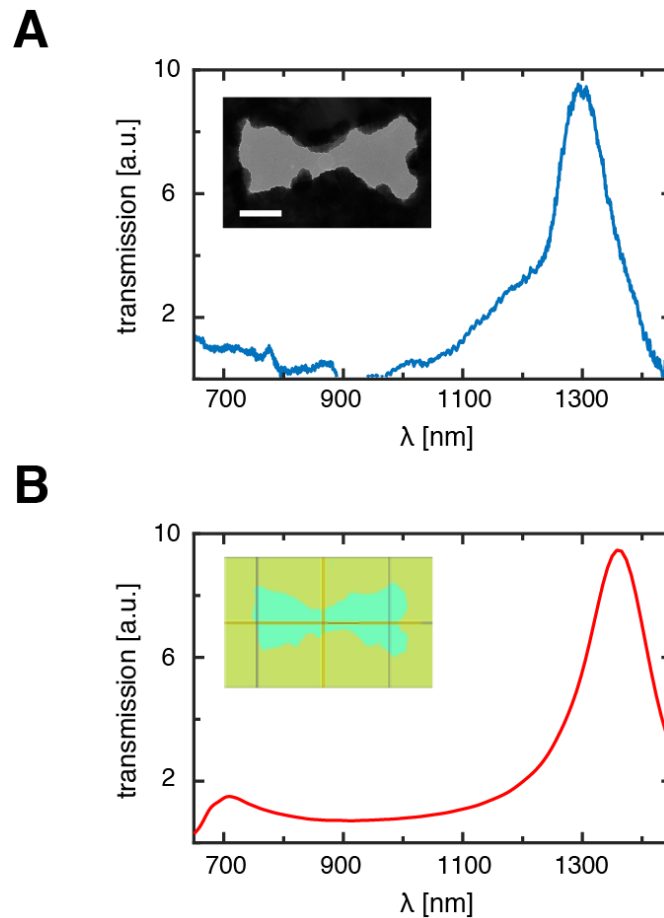


Figure S2. Experimental and simulated transmission spectrum. (A) Experimental transmission spectrum from the nanostructure shown in the inset (scale bar is 50 nm). (B) Simulated transmission spectrum from the nanostructure in (A). The inset shows a top down view of the geometry that was simulated, which was extracted from the TEM image in (A).

Figure S2 show the experimental (A) and simulated (B) transmission spectrum of the nanoantenna, which is shown in the inset of (A). A clear resonance peak can be observed experimentally around 1300 nm (Fig. S2A) and around 1350 nm in the simulated spectrum (Fig. S2B), demonstrating good agreement. Experimental spectra are obtained by inserting the plasmonic nanopore chip in a custom-made flow cell that exposes the nanostructure to ddH₂O and leaves the opposite site exposed to air. The sample is then illuminated by a broadband lamp and a region of interest of 2 μm in size is selected on the sample using a 40 μm circular pinhole in a conjugate image plane. Subsequently, the transmission light collected through the pinhole

is focused onto a spectrometer (Acton SP500i, Princeton Instruments). A spectrum from the nanostructure is obtained by subtracting the averaged background from 8 locations surrounding the nanoantenna from the raw sample spectrum and dividing the result by the spectral intensities of the lamp.

S3. Simulation of idealized inverted-bowtie nanoantenna in transverse polarization

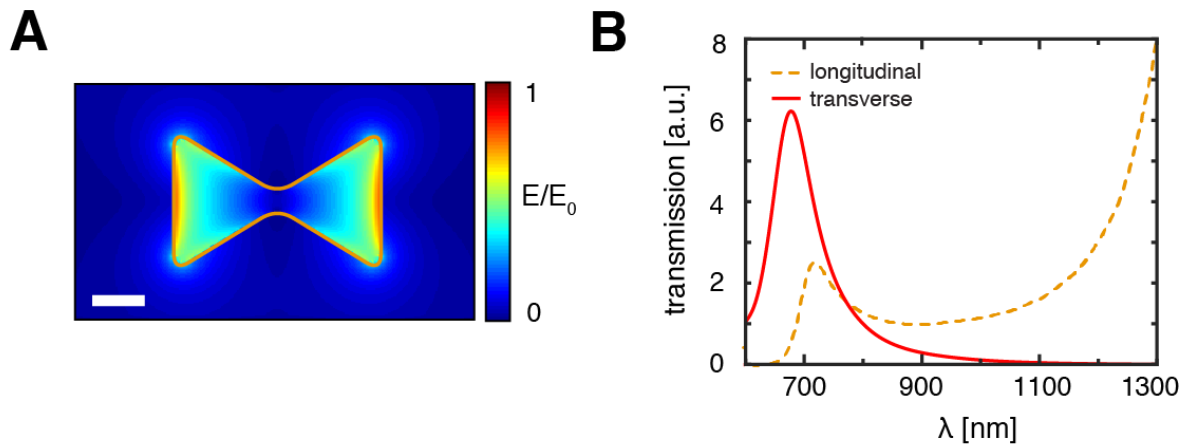


Figure S3. Simulated optical response of the inverted-bowtie nanoantenna.

(A) Normalized electric field density distribution under transverse illumination. No strong optical field enhancement is observed, and in a field density *minimum* can be found in the gap region. Scale bar is 40 nm, (B) Simulated light transmission spectra of the nanostructure under longitudinal and transverse illumination.

S4. Experimental and simulated temperature increase in a plasmonic nanopore

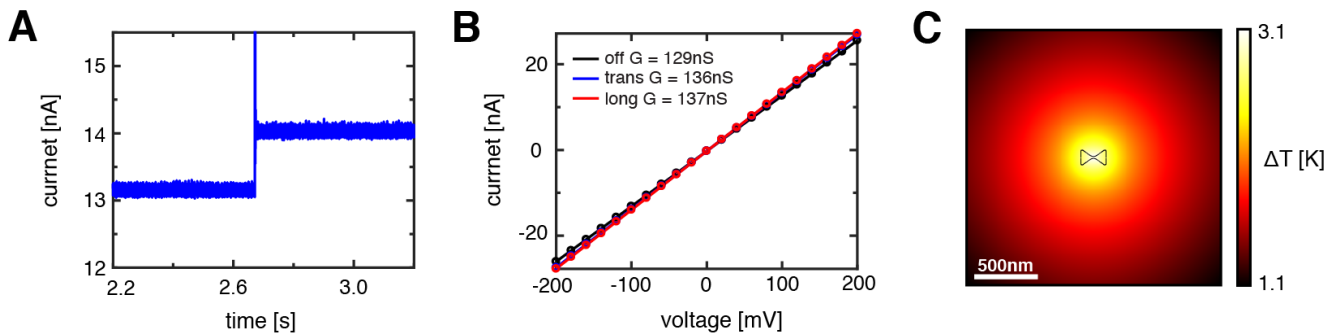


Figure S4. Heating in a plasmonic nanopore. (A) Ionic current increase upon 7.5 mW of laser power in longitudinal mode through a 20 nm plasmonic nanopore at 100 mV and 2 M LiCl. (B) IV characteristics of the same nanopore without laser illumination ($G = 129$ nS) transverse illumination of 7.5 mW ($G = 136$ nS) and longitudinal illumination of 7.5 mW ($G = 137$ nS). (C) Simulated spatial temperature distribution for a heat input equivalent to 7.5 mW of laser illumination in longitudinal mode. Note that the temperature increase amounts to only a modest 3.6°C.

Plasmonic heating due to resistive losses in the metal are a common side effect in plasmon excitation. The plasmonic nanopore naturally allows for the heating to be quantified experimentally, as the nanopore serves as a local temperature probe.¹ A temperature increase leads to an increase in the buffer conductivity, which can be monitored through the nanopore current and as such the nanopore serves as a local thermometer. Indeed, upon laser illumination of a plasmonic nanopore, an increase in the ionic current can be readily observed (Fig. S4A). Figure S4B shows the IV characteristics of the plasmonic nanopore under different illumination conditions. In longitudinal mode under 7.5 mW of illumination power at 1064 nm, a relative current increase of 5.7% is observed, corresponding to a temperature increase of 3.6°C.¹

The temperature increase in a plasmonic nanopore can be modeled using simple finite-element modeling. We used COMSOL Multiphysics 4.0 to simulate the heating in the plasmonic nanoantenna and calculated the resulting temperature increase by setting a fixed total heat power on the surface of the nanoantenna (absorption of plasmonic nanoantenna). Details on the

COMSOL simulation setup can be found elsewhere.² Using an absorption cross-section of 10^{-14} m^2 for the antenna at 1064 nm, as determined through FDTD simulations, a diffraction-limited laser-spot size (objective NA 1.2), and a transmission efficiency through the objective of 50%, 64 μW of the 7.5 mW incident laser power is converted to heat in the plasmonic nanoantenna. This leads to a predicted temperature increase of 3.1°C, which is in good agreement of the 3.6°C observed experimentally. We note that this temperature increase is significantly less than is observed for a nanoantenna dimer, such as the plasmonic bowtie,² which can be attributed to the good heat conductive properties of the gold film.

S5. Blockade current *versus* dwell time scatter plots

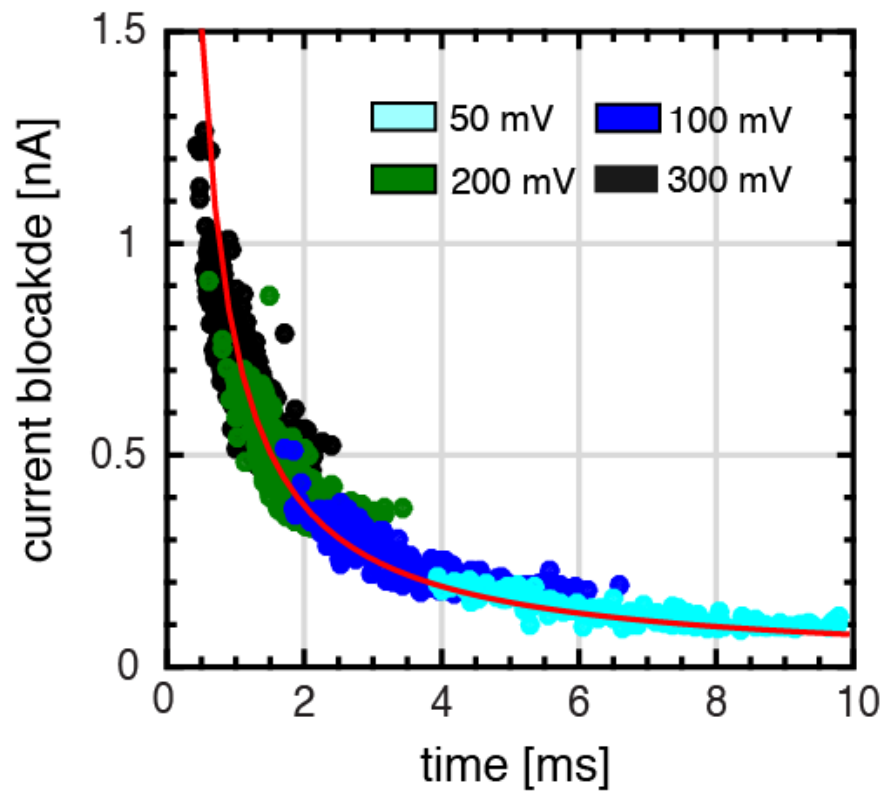


Figure S5. Blockade current *versus* dwell times scatter plot at 50, 100, 200, and 300 mV. The red line is the constant charge deficit contour: average event amplitude \times dwell time = 0.76 ms \cdot nA, as determined from the charge deficit peak of all data points. The data points per voltage scatter in a characteristic L-shape, that follows the constant charge deficit contour. A clear shift in both amplitude and dwell time can be observed.

S6. All-point histograms of optically detected events at different bias voltages

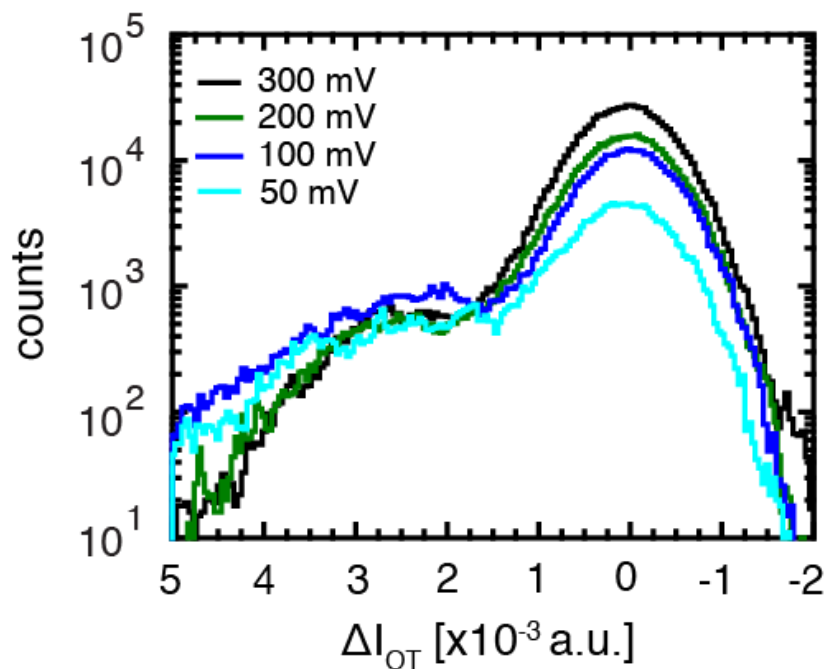


Figure S6. All point histogram from all optically detected events used to determine the signal amplitude at various voltages (Fig. 3c in the main text). Two peaks can be observed, one around 0 (open pore) and one around ~ 2.3 (where two dsDNA strands are inserted into the pore).

S7. Simulation of the normalized electric field across the gold nanoantenna gap

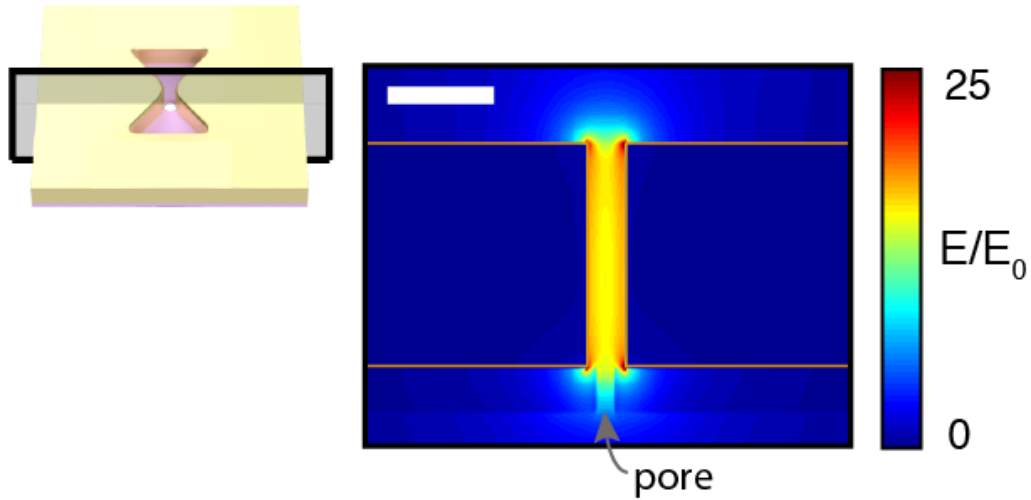


Figure S7. Normalized electric field map of the inverted bowtie excited in longitudinal mode excitation at 1064 nm in the plane indicated in the left inset (*i.e.*, the cross section through the thickness of the gold). The electric field localization extends along the entire thickness of the gold and is approximately uniform in the gap. Scale bar is 50 nm.

S8. Details on the determination of the relative simulated signal amplitude

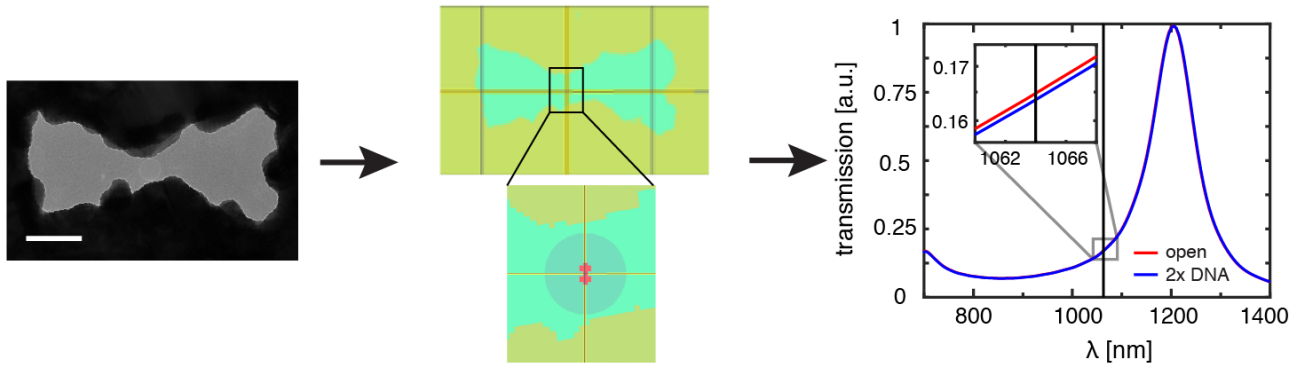


Figure S8. Workflow in determining the simulated signal amplitude. A TEM image is converted into a model shape and the difference in simulated transmission with and without two double strands of DNA is extracted at 1064 nm. The scale bar is 50 nm.

To extract a simulated signal amplitude, we directly simulated the nanoantenna shape as deduced from the TEM image. First a TEM images of the nanostructure is imported into the Lumerical FDTD software using image import. Using thresholding the image is converted into a 2D geometry that can be used in the simulation, and the geometry is perforated through a 100 nm thick gold layer to create the gold nanoaperture. Subsequently the structure is aligned with a 20 nm nanopore (shown in the middle zoom) in the simulation. Two simulations are done: one for an empty pore, and one where the pore contains two strands of dsDNA (as shown in red), simulated as two 200 nm long rods of 2.2 nm in diameter and a refractive index of 2.5. The strands are placed ± 2 nm from the center of the nanopore, in the longitudinal direction. The different simulation spectra for the structure with or without DNA are normalized to the peak transmission intensity, plotted, and the difference is extracted at 1064 nm and divided by the light transmission through the open nanostructure.

We tested the dependence on the exact location of the DNA strand in the nanopore. For this, we used the idealized geometry, as described in the main text. Figure S9 shows the resulting simulated signal amplitude when a single DNA rod is placed at different locations in the nanopore. The DNA rod is moved from the center of the pore to the very edge of the gap of the gold surface. The signal amplitude increases when the DNA moves closer to the surface, but

only very modestly, with an amplitude increase only about 30% from the center to the edge. We thus conclude that the exact position of the DNA is of minor influence to the simulation results. Furthermore, we tested a difference between one and two DNA double strands in the nanopore in the idealized geometry. The normalized amplitude for one DNA rod was 0.00115 at the center and 0.00193 for two rods in the configuration described above.

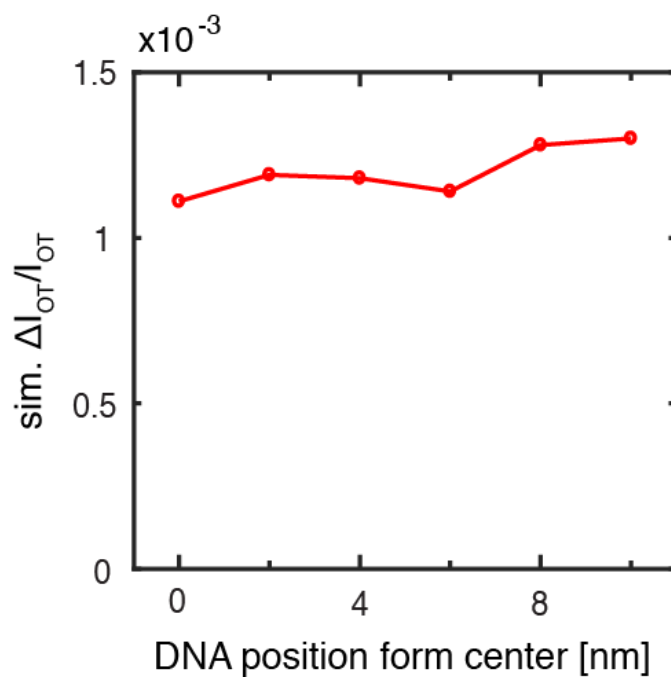


Figure S9. Normalized simulated signal amplitude of one double strand of DNA inserted in a 20 nm pore at different positions from the center. The signal strength is about 30% larger when the DNA strand touches the gold surface than when it is placed at the center.

References

1. Verschueren, D. V.; Jonsson, M. P.; Dekker, C., Temperature Dependence of DNA Translocations through Solid-State Nanopores. *Nanotechnology* **2015**, *26*, 234004.
2. Nicoli, F.; Verschueren, D.; Klein, M.; Dekker, C.; Jonsson, M. P., DNA Translocations through Solid-State Plasmonic Nanopores. *Nano Lett.* **2014**, *14*, 6917-6925.